

Interfacial feedback dynamics in polymer light-emitting electrochemical cells

J. C. deMello*

Centre for Electronic Materials and Devices, Imperial College, Exhibition Road, South Kensington, London SW7 2AY

(Received 6 March 2002; revised manuscript received 16 July 2002; published 31 December 2002)

We present modeling studies to demonstrate how incorporating ions into organic light-emitting diodes improves carrier injection. The simulations show that the electric potential is dropped preferentially at the electrodes, thereby narrowing injection barriers. The studies provide insight into the interfacial feedback dynamics that regulate carrier injection and are relevant to the optimization of light-emitting electrochemical cells for display purposes.

DOI: 10.1103/PhysRevB.66.235210

PACS number(s): 78.20.Jq, 78.60.Fi, 78.66.Qn

Luminescent polymers are of interest owing to their potential use in thin-film emissive displays.¹ High power efficiency is important in these devices, and an interesting technique for achieving this has been reported by Pei *et al.*, in which mobile ions are incorporated into the polymer layer.² Devices formed by sandwiching the ion/polymer layer between two electrodes show low threshold voltages for light emission that are broadly independent of the work functions of the electrodes. More generally, the operation of these light-emitting electrochemical cells (LEC's) is of considerable interest owing to their properties as mixed ion-electron conductors.^{3,4}

It is generally agreed that the low threshold for charge injection results from movement of the mobile ions towards the electrodes, but there is some disagreement in the literature about the role of the ions.^{2,5-7} We have previously used Debye-Huckel theory to show how the accumulation of uncompensated ions near the electrode-polymer interfaces screens the bulk polymer from the external field and reduces the interfacial barrier widths for charge injection.⁶ Under an applied external field, the anions drift to the positive electrode and the cations drift to the negative electrode until drift and diffusion currents are equalized. Because the density of ionic charge is very high ($>10^{25} \text{ m}^{-3}$), small movements of these ions can give rise to very large electric fields. Under conditions of constant applied bias, ionic charge redistribution occurs throughout the bulk of the polymer film until the local electric field has been canceled everywhere. A finite electric field can only be sustained at the interfaces, where the motion of the ions is blocked by the electrodes; since the entire potential is developed in thin layers adjacent to each electrode, the electric fields at the contacts are extremely high (typically 10^9 V m^{-1}). Consequently, the tunneling barriers for electrons and holes are extremely thin and both carrier types can be injected with near 100% efficiency (ensuring high electroluminescence efficiencies). Transport of electronic charges through the field-free bulk is mediated solely by diffusion.^{6,7} This electrodynamic description is able to account for the key physical properties of LEC's, including turn-on biases close to the optical gap, high device efficiencies, and symmetrical current-voltage characteristics. The key assumption of the model is that the polymer bulk remains largely field-free (with the potential being preferentially dropped at the interfaces) even under conditions of relatively high electronic carrier injection. (This contrasts

with the electrochemical models of Pei and Smith in which the electric field is largest at a "junction region" in the center of the device even at low applied biases.^{2,5})

The field-free assumption has been confirmed experimentally for biases up to and including the polymer band gap,⁸ but for higher biases measurements have been inconclusive. It is clear, however, that the field-free regime cannot pertain indefinitely: at sufficiently high biases, the quantity of dissolved ions will be insufficient to fully screen the external field or maintain complete ion-electron compensation in the bulk. Under these conditions bulk transport of electrons and holes will occur under the influence of diffusion *and* drift—as with a conventional organic light-emitting diode (LED). The actual bias at which the field-free regime breaks down depends intimately on the behavior of the charge carriers in the high-field interfacial regions: if a feedback process occurs such that the effective impedances of the interfaces increase in sympathy with the density of injected carriers (thereby regulating the rate of carrier injection), the field-free regime may extend to relatively high biases; if no such feedback mechanism is present, the field-free regime will break down shortly above the threshold for carrier injection. The behavior of the ions and electrons in the high-field interfacial layers is therefore crucial to understanding LEC device operation. To date, however, there has been little if any discussion of this issue in the literature, and it therefore remains an open question whether the field-free regime pertains under ordinary operating conditions.

Since the high-field layers are typically no more than 5–10 Å in thickness, spectroscopic techniques such as charge modulation spectroscopy cannot be used to investigate the electronic carrier densities in the interfacial layers. Indeed, it is doubtful whether any experimental procedure could reliably monitor the electronic carrier concentrations in such a thin layer. In this paper, we use modeling studies to investigate device operation but, in contrast with previously reported work,^{6,7} we make no assumptions about the magnitude of the electric field anywhere in the device. In effect, the LEC is treated as a conventional organic LED that also happens to contain a *fixed quantity of mobile fully dissociated chemically inert ions*. We assume the semiconducting polymer has a negligible intrinsic carrier density, is trap-free, and that carrier mobilities are independent of the internal electric field. The organic film has a thickness d , the anode is located at $x=0$, and the cathode at $x=d$ (see inset to Fig. 1). We

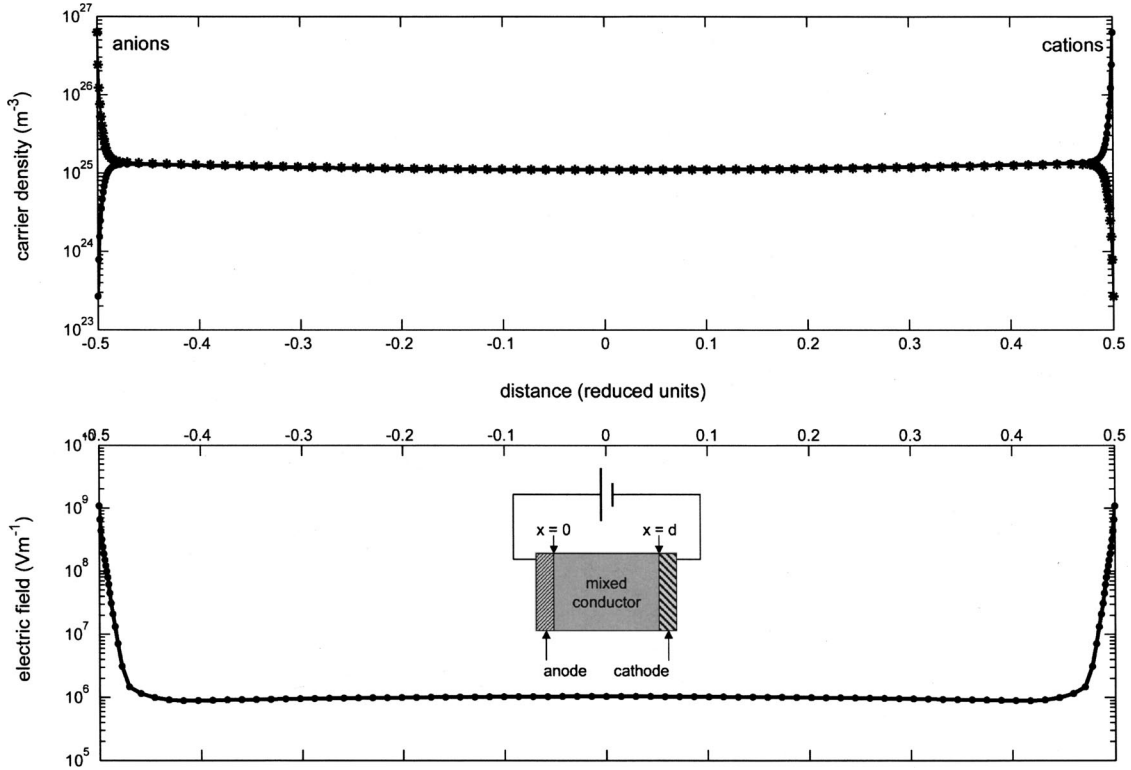


FIG. 1. Ion and field distributions in an LEC of width 3500 Å, assuming an average ion density of $1.25 \times 10^{25} \text{ cm}^{-3}$, equal carrier mobilities ($10^{-6} \text{ m}^2/\text{V s}$), equal injection barriers for electrons and holes ($\Delta\phi=0.5 \text{ eV}$), and a potential difference between anode and cathode of 2 V. Sheets of uncompensated ions accumulate in the vicinity of the electrodes, where motion of the ions is blocked by the electrodes, giving rise to extremely high electric fields. The high fields in turn permit efficient injection of electrons and holes. The x -axis is expressed in reduced coordinates of $\chi=(x-d)/2$, where $\chi=-0.5$ corresponds to the anode and $\chi=0.5$ corresponds to the cathode.

assume that injection of electrons and holes is mediated by a Fowler-Nordheim tunnelling process⁹ with the carrier density falling to zero at the counter electrode, although the precise nature of the injection mechanism does not affect the broad conclusions of this work. The contacts are taken to be ionically blocking—meaning the anion and cation fluxes are zero at each electrode. We further assume that bulk transport of all charge carriers (electrons and ions) is governed by the standard drift-diffusion equations and electron-hole recombination occurs via a Langevin process. The profile of the electric potential is determined from Poisson’s equation. These assumptions are stated mathematically in Eqs. (1)–(7):

$$\frac{\partial n_e}{\partial t} = \mu_e \left[\left(\frac{kT}{e} \right) \nabla^2 n_e - n_e \nabla^2 \phi - (\nabla n_e)(\nabla \phi) \right] - k_{\text{eh}} n_e n_h, \quad (1)$$

$$\frac{\partial n_h}{\partial t} = \mu_h \left[\left(\frac{kT}{e} \right) \nabla^2 n_h + n_h \nabla^2 \phi + (\nabla n_h)(\nabla \phi) \right] - k_{\text{eh}} n_e n_h, \quad (2)$$

$$\frac{\partial n_a}{\partial t} = \mu_a \left[\left(\frac{kT}{e} \right) \nabla^2 n_a - n_a \nabla^2 \phi - (\nabla n_a)(\nabla \phi) \right], \quad (3)$$

$$\frac{\partial n_c}{\partial t} = \mu_c \left[\left(\frac{kT}{e} \right) \nabla^2 n_c + n_c \nabla^2 \phi + (\nabla n_c)(\nabla \phi) \right], \quad (4)$$

$$j_h^0 = + \frac{A(E^0)^2}{\Delta\phi_h} \exp \left\{ \frac{-8\pi\sqrt{2em}}{3h} \frac{\Delta\phi_h^{3/2}}{E^0} \right\},$$

$$j_e^d = - \frac{A(E^d)^2}{\Delta\phi_e} \exp \left\{ \frac{-8\pi\sqrt{2em}}{3h} \frac{\Delta\phi_e^{3/2}}{E^d} \right\}, \quad (5a,5b)$$

$$\nabla n_h|_{x=0} = \frac{e}{kT} (n_h^0 E^0 - j_h^0 / e \mu_h),$$

$$\nabla n_e|_{x=d} = \frac{-e}{kT} (n_e^d E^d + j_e^d / e \mu_h), \quad (6a,6b)$$

$$\nabla^2 \phi = \frac{-e}{\epsilon} (n_h + n_c - n_e - n_a), \quad (7)$$

where ϕ is the electric potential; E is the electric-field strength; n , μ , and j refer, respectively, to the concentrations, mobilities, and fluxes of the charge carriers; the subscripts e , h , a , and c signify electrons, holes, anions, and cations, and the superscripts 0 and d refer to quantities evaluated at the anode and cathode, respectively. k_{eh} is the Langevin electron-hole recombination rate and we have assumed the Einstein relationship between diffusivity and mobility to apply. $\Delta\phi_e$ and $\Delta\phi_h$ are the barrier heights for electron and hole injection (expressed in eV), and A is a proportionality constant that allows for backflow.¹⁰ It should be stressed that

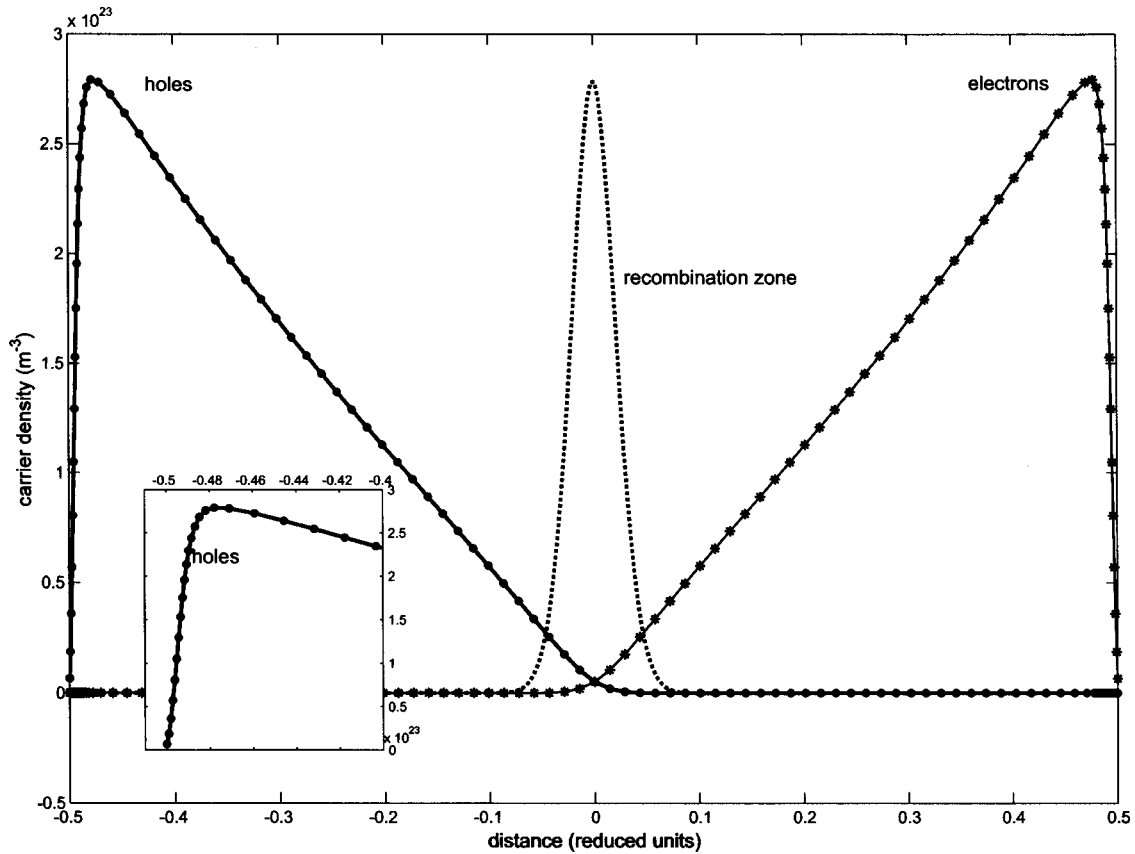


FIG. 2. The electronic charge distributions in the device of Fig. 1. The increase in electron and hole density away from the anode and cathode causes a diffusive countercurrent in the direction of the injecting contact which opposes the large forward moving drift current. In the bulk of the device, charge transport is entirely diffusive and the electron and hole distributions decrease approximately linearly with distance from the parent electrode towards zero in the center of the device. The dotted line indicates the profile of the recombination zone.

we do *not* assume *a priori* the existence of a field-free bulk; rather, the system of equations is allowed to evolve from an arbitrary starting point (constant electric field; no electrons or holes; and homogeneous distributions of anions and cations) until a self-consistent steady-state solution obtains. The system of differential equations is exceptionally stiff owing to extremely steep solution fronts in the interfacial regions, so it is important to use robust numerical routines: we use an adaptive-grid method-of-lines solution procedure based on equidistribution criteria, developed specifically for this purpose.¹¹ The device parameters were: $\epsilon_r = 3.4$, $d = 3500 \text{ \AA}$, $\mu_e, \mu_h = 10^{-6} \text{ m}^2/\text{V s}$, $\phi_0 - \phi_d = 2 \text{ V}$, $\Delta\phi_e, \Delta\phi_h = 0.5 \text{ eV}$, and $\langle n_a \rangle, \langle n_c \rangle = 1.25 \times 10^{25} \text{ m}^{-3}$. Hence we have assumed for convenience a highly symmetric device structure, in which the barriers to electron and hole injection are equal, and electron and hole mobilities are matched; additionally, by equating the potential difference between anode and cathode ($\phi_0 - \phi_d$) with the applied bias, we have implicitly assumed that ξ_0 and ξ_d —the Fermi levels (or chemical potentials) of the anode and cathode—are identical;¹² in other words, we have assumed identical electrode materials for anode and cathode. This is the case for example for planar LEC's fabricated on interdigitated electrodes (assuming no chemical reactions at the electrode-semiconductor interfaces), as reported by Pei.² It should be noted that all of these assumptions may be relaxed without

affecting the broad conclusions of this work. In particular for dissimilar electrode materials, equilibration of the Fermi levels (at zero bias) will generate a reverse internal field, which must be subtracted from the applied bias to determine the potential difference across the device. In other words, $(\phi_0 - \phi_d) = V_{\text{applied}} + (\xi_0 - \xi_d)/e$.

We note that, since the ion fluxes equal zero in steady state and we have assumed Einstein's relation to apply, the mobilities of the ions do not affect the steady-state solutions. The simulations were carried out at a notional temperature of $T = 2500 \text{ K}$ which, although clearly much higher than room temperature, was necessary to *diffusion broaden* the spatial features and make the problem numerically tractable (by lessening the overall stiffness of the system of equations). Similarly, the applied bias of 2 V was somewhat lower than typical operating biases (3–4 V), and the anion and cation concentrations were limited to $1.25 \times 10^{25} \text{ m}^{-3}$ to ease numerical convergence: in real LEC's the ion density can be as high as 10^{27} m^{-3} .² The use of these “unrealistic” parameter values does not affect the general features or appearance of the solution, although it does yield solution fronts that are somewhat shallower than would otherwise be obtained: e.g., for realistic parameter values, the high-field regions will be a bit thinner ($\sim 20\text{--}30\%$) than the simulations reported here would suggest.

In Figs. 1 and 2 we show the steady-state electric-field,

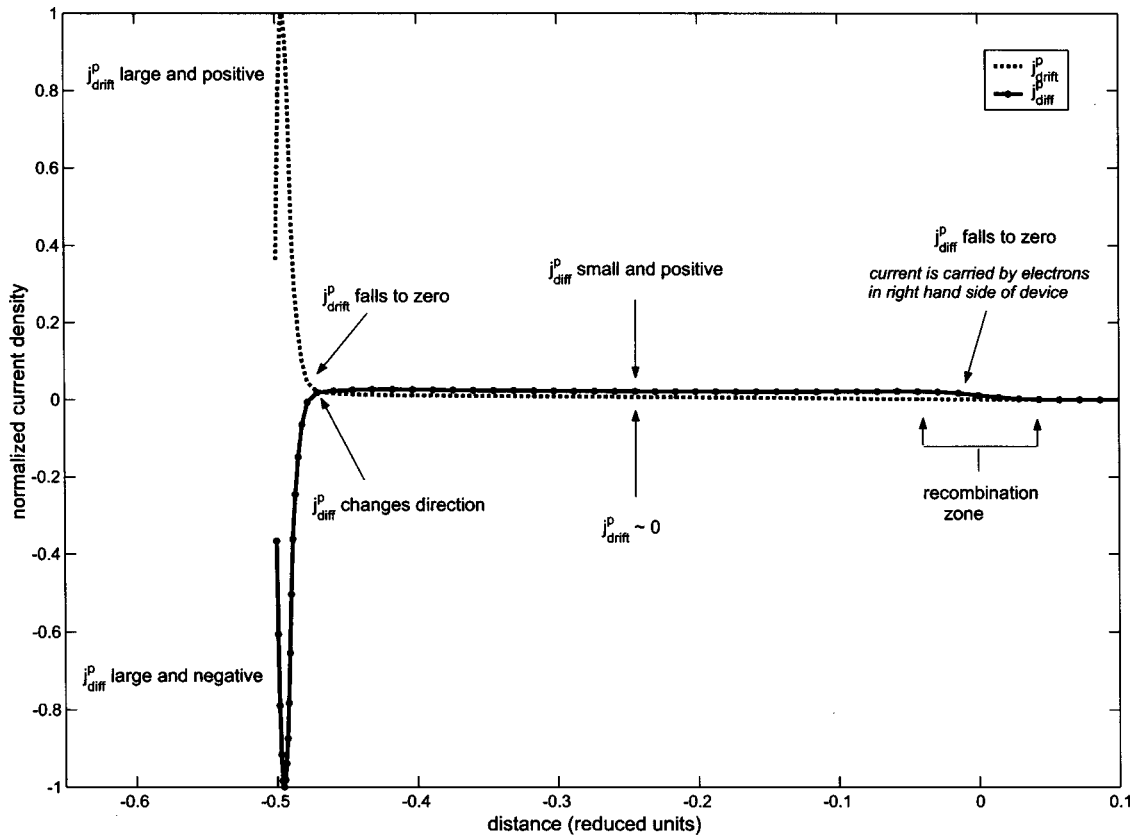


FIG. 3. Variation in the hole drift and diffusion currents away from the anode for the device of Fig. 1. The diffusion current is in the counter direction (i.e., towards the electrodes) in the immediate vicinity of the electrode, and regulates the rate of carrier injection. The drift and diffusion currents of the electrons (not shown) mirror this behavior away from the cathode.

ion-, and electron-distributions for an LEC containing 1.25×10^{25} dissociated ions per cubic meter. From Figs. 1(a) and (b), it can be seen that uncompensated ions accumulate at the two interfaces and screen the external field effectively, with almost the entire electric potential being dropped in two ~ 10 Å layers near to the anode and cathode. The thin interfacial barriers enable easy charge injection via tunneling and, for the parameter values stated above, the steady-state current density is $\sim 55\,000$ A/m². In the absence of the ions, the potential would vary linearly across the device (constant electric field) and the triangular injection barriers would be of thickness $d\Delta\phi_e/(\phi_0 - \phi_d) \sim 875$ Å. Hence there would be a negligible tunneling current through the barrier (although in reality one would expect a contribution to the overall current from thermionic emission which is not explicitly considered in the simulations reported here). The sheets of ions that accumulate at each interface are therefore fundamental to achieving efficient carrier injection in LEC's.

Figure 2 shows the electron and hole distributions. In the bulk of the device, the electron and hole concentrations fall linearly with distance from a maximum close to the parent electrode to zero at the device center (the recombination zone). This behavior is a direct consequence of diffusive transport and has been discussed extensively in the literature.^{3,4,6,7} The profile of the electronic carriers in the high-field regions, however, is interesting. In the immediate vicinity of each electrode, the density of the injected charge

carriers is seen to increase steeply until reaching a maximum value at the far side of the high-field layer (see inset). This contrasts with ordinary organic LED's for which the carrier density is greatest at the injecting contact and decreases into the bulk.¹³

The increase in carrier density away from the contact is fundamental to the operation of the devices and can be understood by, for example, analyzing the hole current near the anode. The hole current in this region can be decomposed into a drift component and a diffusive component. Since the electric field is very high near the injecting contact, the drift current will be extremely large. The bulk semiconductor is unable to sustain a current of this size owing to the low mobilities of the electrons and holes. Therefore, in order to accommodate current conservation throughout the device and compensate for the extremely large (forward-moving) drift current near the anode, the diffusive current in the high-field region must be in the reverse direction and of almost identical magnitude: hence ∇n_h will be positive and the carrier density must increase away from the contact. (An analytical approximation for the carrier profiles in the immediate vicinity of the electrodes may be obtained by equating the drift and diffusive currents which for holes yields the expression $n_h = n_h^0 \exp[-e\{\phi_0 - \phi\}/k_B T]$). In some sense this is the "reverse analog" of *extreme* space-charge limited LED's where the electric field (and hence drift current) changes sign

in the vicinity of the injecting electrode to compensate a large forward-moving diffusive current.¹³

The delicate interplay between diffusive and drift currents in the interfacial regions regulates the overall rate of carrier injection. The carrier densities at the contacts are set by the injection process. As the applied bias is increased, the carrier density at the contact rises sharply, but the diffusive current also increases in direct proportion: the forward-moving drift current is cancelled almost exactly by the diffusive counter-current and therefore the net (forward-moving) current is many orders of magnitude smaller than the drift current next to the electrode. Figure 3 shows the variation in drift and diffusive hole currents through the device; the forward-moving drift current is largest in the high-field layers and very small in the field-free bulk; the diffusive current by contrast is large and negative in the interfacial layers and small and positive in the bulk; the total steady-state device current $i_{\text{tot}} = e\{(j_h^{\text{diff}} + j_h^{\text{drift}}) - (j_e^{\text{diff}} + j_e^{\text{drift}})\}$ is obviously constant throughout.

Riess and Cahen have previously proposed a similar model for device operation.^{4,7} In common with the model reported here, they consider a regime in which the bulk semiconductor is field free and electronic carrier transport is driven by diffusion. The *bulk* electron and hole distributions they obtain are qualitatively similar to those reported here, with the electron and hole densities falling (approximately) linearly with distance from the parent electrode to (approximately) zero at the device center. The precise functional forms of the electron and hole profiles differ for the two models owing to slight differences in approach: here we consider the current in the device to be fixed by carrier injection at the electrodes; Riess and Cahen consider the current to be fixed by the bulk resistance and an Ohmic contact resistance (above a threshold voltage). However, these are relatively small differences and, in the bulk of the device, both models yield broadly similar results. The main additional consideration in the present work is the explicit inclusion of the high-field regions close to each electrode.

The model outlined here contrasts with that of Smith.⁵ He assumes that above a critical bias ϕ_{critical} —which is smaller than the band gap of the polymer—the anions and cations ions in the bulk of the structure spatially separate, thereby forming a “junction region” in which ion-electron compensation does not occur. The surplus bias $\phi_{\text{surplus}} = \phi_0 - \phi_d - \phi_{\text{critical}}$ is dropped exclusively at this non-neutral junction

region with the remainder of the bulk remaining field free. This behavior arises in part from the assumption of a low free-ion concentration, which in turn follows from his assumption of strong binding between the anions and cations. Smith does not consider in any detail the interfacial regions.

Finally, we note that in this paper we have considered extrinsic carrier densities that are small in relation to the number of ions present. As mentioned earlier, at sufficiently high biases, the assumption of a field-free bulk will certainly break down. The simulations indicate that this will occur when the average concentration of electrons or holes exceeds about five percent of the average ion concentration. The corresponding current density may be determined from Fick’s law: if the density of ions is 10^{27} m^{-3} , the device width is 2000 \AA , and the electron and hole mobilities are $10^{-10} \text{ m}^2/\text{Vs}$, the ratio of electrons to ions will exceed five percent at a current density of 200 A m^{-2} , which is readily achieved in a real device. (For higher electron and hole mobilities, larger current densities will be permissible before the field-free assumption breaks down.) We defer detailed discussion of this regime to a later paper but note that—in contrast to the electrochemical models of Pei and Smith^{2,5}—the excess electric potential is dropped across the entire polymer bulk and does not appear preferentially in a junction region.

In conclusion, we have shown phenomenologically how the incorporation of ions into a conventional LED leads to significant improvements in carrier injection. The modelling studies treat the LEC as a conventional injection-limited organic LED that also happens to contain a fixed quantity of fully dissociated chemically inert ions. The simulations—which make no *a priori* assumptions about the electric-field distribution—support previous studies and in particular confirm that the electric potential is dropped preferentially at the electrodes, thereby narrowing barriers to carrier injection. (This contrasts with the electrochemical models of Pei and Smith in which the electric field is largest at a “junction region” in the center of the device.^{2,5}) The studies provide insight into the interfacial feedback dynamics that regulate carrier injection and are relevant to the optimization of LEC’s for display purposes. The results are also of interest in the general area of mixed ion-electron conduction and especially for microbatteries where (inorganic) mixed conductors are attractive materials for intercalation electrodes owing to Wagner enhancement of ion mobilities.³

*Email address: j.demello@ic.ac.uk

¹J. H. Burroughes *et al.*, Nature (London) **347**, 539 (1990).

²Q. B. Pei *et al.*, Science **269**, 1086 (1995).

³W. Weppner, in *Solid State Electrochemistry*, edited by P. G. Bruce (Cambridge University Press, Cambridge, 1995), p. 199.

⁴I. Riess, J. Phys. Chem. Solids **47**, 129 (1986).

⁵D. L. Smith, J. Appl. Phys. **81**, 2869 (1997).

⁶J. C. deMello *et al.*, Phys. Rev. B **57**, 12 951 (1998).

⁷I. Riess and D. Cahen, J. Appl. Phys. **82**, 3147 (1997).

⁸J. C. deMello *et al.*, Phys. Rev. Lett. **85**, 421 (2000).

⁹R. H. Fowler and L. Nordheim, Proc. R. Soc. London, Ser. A **119**, 173 (1928).

¹⁰P. S. Davids *et al.*, Appl. Phys. Lett. **69**, 2270 (1996).

¹¹J. C. deMello, J. Comput. Phys. **181**, 564 (2002).

¹²I. Riess, Solid State Ionics **95**, 327 (1996).

¹³P. A. Torpey, J. Appl. Phys. **56**, 2284 (1984).